J. Fluid Mech. (1992), *vol.* 241, *pp.* 109–123
Printed in Great Britain

Instability of unbounded uniform granular shear flow

By S. B. SAVAGE

Department of Civil Engineering and Applied Mechanics, McGill University, Montreal H3A 2K6, Canada

(Received 19 March 1991 and in revised form 13 January 1992)

The paper presents a linear stability analysis of cohesionless granular materials during rapid shear flow. The analysis is based on the governing equations developed in the kinetic theory of Lun *et al.* (1984) for granular flows of smooth, nearly elastic, uniform spherical particles. The primary flow is taken to be a uniform, simple shear flow and the effects of small perturbations in velocity components, granular temperature and solids fraction are considered. The inelasticity of the particles is characterized by a constant coefficient of restitution which is assumed to be close to unity. Some permissible solutions are sinusoidal plane waves in which the wavenumber vector is continuously turned by the mean shear flow and its magnitude varied as time proceeds. The initial growth (or decay) rates for these perturbations are sought. The resulting linearized equations for the flow perturbations turn out to be exceedingly long and complex; they are determined by the use of computer algebra. It is found that, in general, long wavelengths are the most unstable and that short wavelengths are dampened by 'viscous action'. 'Instability' increases with decreasing coefficient of restitution. Numerical results for initial growth rates were obtained for several values of mean solids fraction and particle coefficient of restitution. Flows tend to be more stable at both high and very low concentrations than at moderate concentrations. These results appear to be consistent in the main with recent computer simulations of granular flows of disk-like particles by Hopkins & Louge (1991).

1. Introduction

There are many scientific and technological problems that involve rapid deformations of granular materials made up of discrete particles. These include mineral, powder and ceramic processing, materials handling engineering, chemical engineering applications of fluidized particles, manufacture of pharmaceuticals, etc. as well as numerous geophysical flows such as rockfalls and avalanches, debris flows, pyroclastic flows, and pack-ice flows. Our present understanding of how these materials behave during flow is still fairly rudimentary compared to that associated with more widely studied single-phase Newtonian and non-Newtonian fluids.

During the past several years there has been considerable effort devoted to the determination of the constitutive behaviour of granular materials by considering the details of the flow at the microstructural level and examining individual particle interactions. Much of this work has dealt with rapid shear flow regimes in which the particle interactions were treated as nearly instantaneous collisions for the purposes of determining overall 'continuum' stresses, energy fluxes, energy dissipation, etc. The studies have been pursued by analytical approaches as well as by means of computer simulations (see review papers by Savage 1983, 1984, 1989, 1991; Jenkins 1987*a*, *b*; Campbell 1990). On the analytical front, the basic ideas of Bagnold (1954) have been extended in much more elaborate approaches patterned after the 'hard-sphere' kinetic theories previously developed for dense gases and liquids (Savage & Jeffrey 1981; Shen & Ackerman 1982, 1984; Haff 1983, 1986; Jenkins & Savage 1983; Lun *et al.* 1984; Jenkins & Richman 1985) and used to study the important problem of boundary conditions (Hui *et al.* 1984; Jenkins & Richman 1986; Gutt & Haff 1988; Richman 1988; Richman & Chou 1988; Haines, Jenkins & Richman 1988). The key difference in the case of granular flows is the inclusion of energy dissipation which occurs during collisions and sliding contacts between rough, inelastic, granular particles. Some important results that emerge from these granular kinetic theories are the evolution equations for the particle velocity fluctuations and spins. The kinetic energy associated with the translational velocity fluctuations has been expressed in terms of a 'granular temperature', which has an obvious analogy with the definition of the temperature in a gas at the molecular level. Because of the significant collisional energy dissipation, shearing is essential to provide the energy necessary to maintain the velocity fluctuations; otherwise the granular temperature quickly decays. This is quite unlike what happens, for example, in a gas at the molecular level.

During the same period, investigations of granular flows have been carried out by computer simulations (Campbell 1989; Campbell & Brennen 1985; Campbell & Gong 1986; Walton & Braun 1986*a*, *b*; Walton *et al.* 1987; Walton, Kim & Rosato 1991; Hopkins & Shen 1988). These simulations have verified some of the general trends which emerge from the kinetic theory analyses, but, more importantly, they have also revealed or confirmed some of the limitations of these kinetic theories and located the flow regimes where the assumptions used in the analyses are inappropriate or break down. Examples of such shortcomings are the assumption of isotropy in the particle radial distribution function at contact and the associated inability to predict particle 'layering' in high concentration shear flows, the assumption of isotropy of the granular temperature, etc.

The kinetic theories have been applied to solve problems in which the spatial and/or temporal variations in the flow field properties were assumed to be (at most) gradual, and the possibility of 'turbulent-like' fluctuations has been neglected. Thus, these analyses have used transport coefficients analogous to laminar flow Newtonian viscosities, thermal conductivity, etc. Until recently, it appeared that computer simulations gave results that were in the main consistent with the kinetic theories and that the differences were due to oversimplifications in the kinetic theories. Most of these computations made use of relatively small numbers of particles and used periodic boundary conditions in an attempt to extend the flow field region effectively. However, there is a small, but growing body of evidence (Hopkins & Louge 1991; Savage 1991; Walton *et al.* 1991) which suggests that under some circumstances the flow fields can depart significantly from the smooth slowly varying ones often assumed.

For example, Savage (1991) found in computer simulations of sheared spherical particles in narrow gaps between rough walls (made up particles similar to those in the shear gap), that in some flow regions turbulent-like flow occurred. For nearly elastic particles, at higher concentrations, the stresses showed strong time-dependent fluctuations; the power spectra of these fluctuations had the form of $1/f$ noise where f is the frequency (Schlesinger & West 1988; Voss 1988). The dynamical system in these computer simulations was also found to be a 'chaotic' one. The granular flow stresses are similar in certain respects to the Reynolds stresses in a turbulent fluid. They depend upon the magnitude of the particle velocity fluctuations, and hence the kinetic energy of the velocity fluctuations. The $1/f$ form of the power spectra of the normal stresses (and hence the kinetic energy of the fluctuations) suggests an analogy with the 'Kolmogorov–Obukov' $-\frac{5}{3}$ law for fluid turbulence. The observed temporal coherence implies the formation of associated spatial structures. Apparently similar stress fluctuations have been observed in shear cell laboratory experiments by Savage & Sayed (1984).

Recently, Hopkins & Louge (1991) have performed computer simulations of two-dimensional granular flows of uniform, smooth, inelastic, circular disks involving large numbers (up to several thousands) of particles. They examined the concentration field using Fourier analysis and found the formation of inhomogeneities, the size and strength of which depended upon the particles' coefficient of restitution, mean solids fraction and the size of the computational region.

It is interesting to note recent work on the development of structures in other areas involving disperse systems. Cluster formation can be seen in computer simulations (Brady & Bossis 1988) and in experiments (Barnes 1989) of low-Reynolds-number sheared suspensions. Internal structures also form during the sedimentation of small bidisperse particles in viscous fluids (Weiland, Fessas & Ramarao 1984; Batchelor & Janse van Rensburg 1986) in fluidized beds (cf. Jackson 1985; Green & Homsy 1987) and three-phase flows (Kytömaa & Brennen 1990). It could well be that inhomogeneities in particulate flows are commonplace.

The appearance of the clustering, stress fluctuations and other inhomogeneities suggests the study of the stability of granular shear flows which are subjected to small disturbances. Apart from the short and restricted analysis in Lun *et al.* (1984) which considered only density perturbations, no such investigations have been performed. The present paper examines the linear stability of a simple uniform shear flow of constant granular temperature and solids fraction when subjected to small perturbations in the mean flow velocity components, the granular temperature and solids fraction. Solutions for the growth (or decay) rates of the perturbations are determined by the use of computer algebra for disturbances of various wavelengths. Qualitative comparisons are made with the computer simulations of Hopkins & Louge (1991) which were performed for two-dimensional flows of smooth disks.

2. Problem formulation and governing equations

2.1. *Conservation and constitutive equations*

We shall consider the linear stability of an unbounded flow at a constant shear rate Γ, uniform granular temperature T and uniform bulk density ρ. Thus, the undisturbed velocity field is given by

$$\boldsymbol{U}(y) = U(y)\,\boldsymbol{e}_x = \Gamma y \boldsymbol{e}_x, \tag{2.1}$$

where $\boldsymbol{e}_x$ is the unit vector in the streamwise x-direction.

We make use of the conservation and constitutive equations developed in the kinetic theory of Lun *et al.* (1984). This theory included collisional as well as kinetic contributions to the transport properties and thus it can be used at both high- and low-solids fractions where these contributions are respectively dominant. The theory was derived for uniform, smooth, spherical particles of diameter σ which were nearly elastic (i.e. the coefficient of restitution $e \approx 1$). The analysis is in effect a perturbation about the perfectly elastic, high granular temperature, small shear-rate limit and the

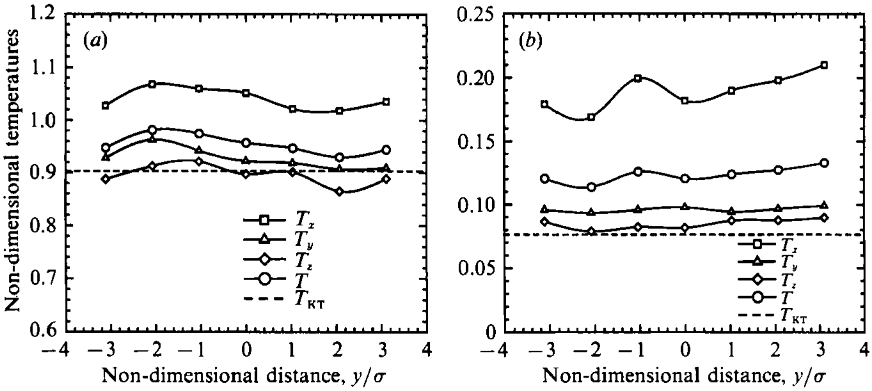

FIGURE 1. Comparisons of granular temperatures determined from molecular dynamics computer simulations with kinetic theory (dashed line) of Lun *et al.* (1984) for a uniform shear flow. Both cases are soft-sphere simulations for a solids fraction $\nu_0 = 0.4712$. (*a*) $e = 0.9$; (*b*) $e = 0.1$.

nearly elastic (small dissipation) condition is required for the theory to be consistent. For example, the assumed form of the velocity distribution function used in Lun *et al.* (1984) forces the granular temperature to be isotropic. While this is quite accurate for nearly elastic particles, it is inadequate for low values of e. To illustrate this, computations were performed using both 'hard-sphere' and 'soft-sphere' computer simulations similar to the approach described in Savage (1991), but with the Lees–Edwards (1972) periodic boundary conditions applied to induce a simple shear flow $U(y) = \Gamma y$. The components of the granular temperature were determined by taking the mean square of the components of the particle velocity fluctuations. For example, $T_x = \langle C_x^2 \rangle$, where $C_x = c_x - U(y)$ is the x-component of velocity fluctuation and c_x is the x-component of the instantaneous particle velocity $\boldsymbol{c}$. Figure 1 compares some typical soft-sphere results (expressed in terms of the non-dimensional variables that are defined subsequently) of computations for 343 particles (an initial cubic array of $7 \times 7 \times 7$ particles) having coefficients of restitution of 0.9 and 0.1, and a mean solids fraction $\nu = 0.4712$. At the higher value of $e = 0.9$ (figure 1) the granular temperatures are approximately isotropic ($T_x \approx T_y \approx T_z \approx T$), but a consistent pattern is observed in that $T_x > T_y > T_z$. The hard-sphere and soft-sphere simulations give approximately the same results and the total granular temperature $T = \frac{1}{3}(T_x + T_y + T_z)$ is only slightly larger than the isotropic value of T predicted for a uniform simple shear flow by the kinetic theory of Lun *et al.* (1984). Note that the temperature scale in figure 1(*a*) is expanded and while the departures from uniformity over the width of the shear region are small, there is some suggestion of sinusoidal temperature variations. By averaging over longer times, for the cases involving relatively small numbers of particles and computational boxes of small lateral dimensions, it is usually possible to eliminate the spatial variations. (Obviously a long averaging time will not always smooth things out; if it could, there would be little point in the present stability analysis.) We have purposely averaged over moderate times in order to reveal the presence of these small granular temperature variations which are similar to the sinusoidal perturbations studied in the present paper. At the lower value of $e = 0.1$ (figure 1*b*), the strong anisotropy in temperature that emerges in the molecular dynamics computations is evident, while the Lun *et al.* (1984) kinetic theory prediction is lower than the total temperature T from the soft-sphere simulation. At low-solids fractions the anisotropies in temperature are even more pronounced for highly dissipative particles. (Note that

Richman (1989) has considered a kinetic theory to predict these kinds of temperature anisotropies for very inelastic particles in the limit of low-solids fractions.) The main purpose of these remarks is to point out that the stability analysis that follows should not be applied to highly dissipative particles, but is probably consistent only for moderate and high values of the coefficient of restitution e.

The equations expressing the conservation of mass, momentum and energy are written in the usual form as

$$\frac{\mathrm{d}\rho}{\mathrm{d}t} = -\rho\nabla\cdot\boldsymbol{u}, \tag{2.2}$$

$$\rho\frac{\mathrm{d}\boldsymbol{u}}{\mathrm{d}t} = \rho\boldsymbol{g} - \nabla\cdot\boldsymbol{p}, \tag{2.3}$$

$$\tfrac{3}{2}\rho\frac{\mathrm{d}T}{\mathrm{d}t} = -\boldsymbol{p}:\nabla\boldsymbol{u} - \nabla\cdot\boldsymbol{q} - \gamma. \tag{2.4}$$

where $\boldsymbol{u} = \langle\boldsymbol{c}\rangle$ is the bulk velocity, $\boldsymbol{p}$ is the stress tensor, and $\boldsymbol{g}$ is the gravitational acceleration. The third equation involves $\frac{3}{2}T = \frac{1}{2}\langle C^2\rangle$, the specific kinetic energy of the velocity fluctuations (where $\boldsymbol{C} = \boldsymbol{c} - \boldsymbol{u}$), the flux of fluctuation energy $\boldsymbol{q}$ and γ, the collisional rate of energy dissipation per unit volume.

Let us now introduce the following non-dimensional time and spatial coordinates

$$(\tilde{t}, \tilde{x}, \tilde{y}, \tilde{z}) = (\Gamma t, x/\sigma, y/\sigma, z/\sigma), \tag{2.5}$$

where σ is the particle diameter. The solids fraction (volume of solids per unit volume) is

$$\nu = \frac{\rho}{\rho_{\mathrm{p}}}, \tag{2.6}$$

where ρ_{p} is the mass density of the individual solid particles. The dimensionless velocity components in the $\tilde{x}$-, $\tilde{y}$-, $\tilde{z}$-directions are defined as

$$(\tilde{u}, \tilde{v}, \tilde{w}) = (1/\sigma\Gamma)(u, v, w), \tag{2.7}$$

and hence the primary non-dimensional mean shear flow is $\tilde{U}(\tilde{y}) = U(y)/(\sigma\Gamma) = \tilde{y}$.

The dimensionless granular temperature, stress, fluctuation kinetic energy flux and rate of collisional energy dissipation are defined as

$$\left.\begin{aligned} \tilde{T} &= \frac{T}{\sigma^2\Gamma^2}, \quad & \tilde{\boldsymbol{p}} &= \frac{\boldsymbol{p}}{\rho_{\mathrm{p}}\sigma^2\Gamma^2}, \\ \tilde{\boldsymbol{q}} &= \frac{\boldsymbol{q}}{\rho_{\mathrm{p}}\sigma^3\Gamma^3}, \quad & \tilde{\gamma} &= \frac{\gamma}{\rho_{\mathrm{p}}\sigma^2\Gamma^3}. \end{aligned}\right\} \tag{2.8}$$

Using the above non-dimensionalizations the conservation equations may be rewritten in dimensionless form as

$$\frac{\mathrm{d}\nu}{\mathrm{d}\tilde{t}} = -\nu\nabla\cdot\boldsymbol{u}, \tag{2.9}$$

$$\nu\frac{\mathrm{d}\tilde{\boldsymbol{u}}}{\mathrm{d}\tilde{t}} = \nu\tilde{\boldsymbol{g}} - \tilde{\nabla}\cdot\tilde{\boldsymbol{p}}, \tag{2.10}$$

$$\tfrac{3}{2}\nu\frac{\mathrm{d}\tilde{T}}{\mathrm{d}\tilde{t}} = -\tilde{\boldsymbol{p}}:\tilde{\nabla}\tilde{\boldsymbol{u}} - \tilde{\nabla}\cdot\tilde{\boldsymbol{q}} - \tilde{\gamma}, \tag{2.11}$$

where $\tilde{\boldsymbol{g}} = \boldsymbol{g}/(\sigma\Gamma^2)$.

All the equations that follow will use non-dimensional variables and for the sake of brevity in notation we shall henceforth omit the tildes. The constitutive relations for non-dimensional stress, translational fluctuation energy flux and the rate of collisional energy dissipation per unit volume are given by

$$\boldsymbol{p} = [F_1(\nu)\,T - \alpha(\nu, T)\,\boldsymbol{\nabla}\cdot\boldsymbol{u}]\,\boldsymbol{I} - F_2(\nu, T)\,\boldsymbol{S}, \tag{2.12}$$

$$\boldsymbol{q} = -K(\nu, T)\,\boldsymbol{\nabla} T, \tag{2.13}$$

$$\gamma = \frac{48}{\pi^{\frac{1}{2}}}\eta(1-\eta)\,\nu^2 g_0\,T^{\frac{3}{2}}, \tag{2.14}$$

where

$$\eta = \tfrac{1}{2}(1+e), \tag{2.15}$$

$$F_1(\nu) = \nu(1+4\eta\nu g_0), \tag{2.16}$$

$$\alpha(\nu, T) = \tfrac{8}{3}\eta\nu^2 g_0\left(\frac{T}{\pi}\right)^{\frac{1}{2}}, \tag{2.17}$$

$$F_2(\nu, T) = \frac{5}{48}\frac{\pi\eta}{\eta(2-\eta)\,g_0}\left(\frac{T}{\pi}\right)^{\frac{1}{2}}(1+\tfrac{8}{5}\eta\nu g_0)\,[1+\tfrac{8}{5}\eta(3\eta-2)\,\nu g_0] + \tfrac{16}{5}\nu^2 g_0\left(\frac{T}{\pi}\right)^{\frac{1}{2}} = F_3(\nu)\left(\frac{T}{\pi}\right)^{\frac{1}{2}}, \tag{2.18}$$

$$K(\nu, T) = \frac{25}{16}\frac{\pi}{\eta(41-33\eta)\,g_0}\left(\frac{T}{\pi}\right)^{\frac{1}{2}} \times\left\{(1+\tfrac{12}{5}\eta\nu g_0)\,[1+\tfrac{12}{5}\eta^2(4\eta-3)\,\nu g_0] + \frac{64}{25\pi}(41-33\eta)\,(\eta\nu g_0)^2\right\}, \tag{2.19}$$

and $\boldsymbol{I}$ is the identity tensor. The rate of shear tensor is defined as

$$\boldsymbol{S} = \tfrac{1}{2}(u_{i,j}+u_{j,i}) - \tfrac{1}{3}u_{k,k}\,\delta_{ij}. \tag{2.20}$$

We use the expression proposed by Carnahan & Starling (1969) for the radial distribution function at contact

$$g_0(\nu) = \frac{(2-\nu)}{2(1-\nu)^3}. \tag{2.21}$$

In the above expression (2.13) for the flux of fluctuation kinetic energy $\boldsymbol{q}$, the term given in Lun *et al.* (1984) that was proportional to $\boldsymbol{\nabla}\nu$ has been omitted, since, as Lun *et al.* point out, it is of higher order than the term proportional to $\boldsymbol{\nabla} T$. Taking $(1-e)$ to be a small parameter and retaining only first-order terms as suggested by Jenkins (1987*b*) we can make the following further simplifications

$$F_1(\nu) = \nu(1+4\nu g_0), \tag{2.22}$$

$$\alpha(\nu, T) = \tfrac{8}{3}\nu^2 g_0\left(\frac{T}{\pi}\right)^{\frac{1}{2}}, \tag{2.23}$$

$$F_2(\nu, T) = \frac{5}{48}\frac{\pi}{g_0}(1+\tfrac{8}{5}\nu g_0)^2\left(\frac{T}{\pi}\right)^{\frac{1}{2}} + \tfrac{16}{5}\nu^2 g_0\left(\frac{T}{\pi}\right)^{\frac{1}{2}} = F_3(\nu)\left(\frac{T}{\pi}\right)^{\frac{1}{2}}, \tag{2.24}$$

$$K(\nu, T) = \frac{1}{g_0}\left\{\frac{25\pi}{128}[1+\tfrac{12}{5}\nu g_0]^2 + 4(\eta\nu g_0)^2\right\}\left(\frac{T}{\pi}\right)^{\frac{1}{2}}, \tag{2.25}$$

and

$$\gamma = \frac{24}{\pi^{\frac{1}{2}}}(1-e)\,\nu^2 g_0\,T^{\frac{3}{2}}. \tag{2.26}$$

2.2. *Linearized small perturbation equations*

If we consider the above granular flow equations for the case of an unbounded uniform shear flow at constant solids fraction ν and constant granular temperature T it is seen that the fluctuation kinetic energy equation (2.11) reduces to a balance between the shear work and γ, the collisional energy dissipation rate per unit volume. This zeroth-order primary flow solution expressed in non-dimensional variables for a particular constant solids fraction ν_0 is found to be

$$T_0 = \frac{F_3(\nu_0)}{48(1-e)\,\nu_0^2 g_0}, \tag{2.27}$$

$$p_{xx_0} = p_{yy_0} = p_{zz_0} = \bar{p}_0 = \nu_0 T_0(1+4\nu_0 g_0), \tag{2.28}$$

$$p_{xy_0} = p_{yx_0} = -\tfrac{1}{2}F_2(\nu_0, T_0), \tag{2.29}$$

recalling that the non-dimensional shear-rate is unity.

We now consider small two-dimensional perturbations about the above solution such that

$$u = U + u'(x,y,t) = y + u'(x,y,t), \quad v = v'(x,y,t), \quad w = 0; \tag{2.30}$$

$$\nu = \nu_0 + \nu'(x,y,t), \quad T = T_0 + T'(x,y,t), \tag{2.31}$$

$$\boldsymbol{p} = \boldsymbol{p}_0 + \boldsymbol{p}'(x,y,t), \quad \boldsymbol{q} = \boldsymbol{q}_0 + \boldsymbol{q}'(x,y,t), \tag{2.32}$$

$$\gamma = \gamma_0 + \gamma'(x,y,t), \tag{2.33}$$

where the primed quantities are small compared with those associated with the primary flow (subscripted 0 quantities).

Substituting (2.30)–(2.33) into the conservation equations (2.9)–(2.11) and collecting first-order terms we obtain the following equations for the perturbation quantities.

$$\frac{\partial \nu'}{\partial t} + U\frac{\partial \nu'}{\partial x} = -\nu_0\left(\frac{\partial u'}{\partial x} + \frac{\partial v'}{\partial y}\right), \tag{2.34}$$

$$\frac{\partial u'}{\partial t} + U\frac{\partial u'}{\partial x} + \frac{\partial U}{\partial y}v' = -\frac{1}{\nu_0}\left(\frac{\partial p'_{xx}}{\partial x} + \frac{\partial p'_{xy}}{\partial y}\right), \tag{2.35}$$

$$\frac{\partial v'}{\partial t} + U\frac{\partial v'}{\partial x} = -\frac{1}{\nu_0}\left(\frac{\partial p'_{xy}}{\partial x} + \frac{\partial p'_{yy}}{\partial y}\right), \tag{2.36}$$

$$\tfrac{3}{2}\nu_0\left(\frac{\partial T'}{\partial t} + U\frac{\partial T'}{\partial x}\right) = -\left(p_{xx_0}\frac{\partial u'}{\partial x} + p'_{xy}\frac{\partial U}{\partial y} + p_{xy_0}\frac{\partial u'}{\partial y} + p_{yx_0}\frac{\partial v'}{\partial x} + p_{yy_0}\frac{\partial v'}{\partial y}\right) - \boldsymbol{\nabla}\cdot\boldsymbol{q}' - \gamma'. \tag{2.37}$$

Making use of (2.31), (2.32) and (2.22)–(2.24) in the stress tensor (2.12) we obtain the following expressions for the perturbation stresses

$$p'_{xx} = F_{1_0}T' + T_0\frac{\partial F_1}{\partial \nu}\bigg|_0 \nu' - (\alpha_0 + \tfrac{2}{3}F_2|_0)\frac{\partial u'}{\partial x} - (\alpha_0 - \tfrac{1}{3}F_2|_0)\frac{\partial v'}{\partial y}, \tag{2.38}$$

$$p'_{yy} = F_{1_0}T' + T_0\frac{\partial F_1}{\partial \nu}\bigg|_0 \nu' - (\alpha_0 - \tfrac{1}{3}F_2|_0)\frac{\partial u'}{\partial x} - (\alpha_0 + \tfrac{2}{3}F_2|_0)\frac{\partial v'}{\partial y}, \tag{2.39}$$

$$p'_{xy} = -\frac{1}{2}\frac{\partial U}{\partial y}\left(\frac{\partial F_2}{\partial \nu}\bigg|_0 \nu' + \frac{\partial F_2}{\partial T}\bigg|_0 T'\right) - \tfrac{1}{2}F_2|_0\left(\frac{\partial u'}{\partial y} + \frac{\partial v'}{\partial x}\right). \tag{2.40}$$

In these equations the subscript 0 denotes dependent variables associated with the undisturbed primary flow (ν_0, T_0, etc.) or functions evaluated using those values.

3. Stability analysis

If we substitute the zeroth-order stress components (2.28) and (2.29) and the perturbation stresses (2.38)–(2.40) in the perturbation momentum and energy equations (2.35)–(2.37) we obtain

$$\nu_0\left(\frac{\partial u'}{\partial t}+U\frac{\partial u'}{\partial x}+\frac{\partial U}{\partial y}v'\right) = F_{1_0}\frac{\partial T'}{\partial x}-T_0\frac{\partial F_1}{\partial \nu}\bigg|_0\frac{\partial \nu'}{\partial x}+(\alpha_0+\tfrac{2}{3}F_{2_0})\frac{\partial^2 u'}{\partial x^2}$$
$$+(\alpha_0-\tfrac{1}{3}\Phi_{2_0})\frac{\partial^2 v'}{\partial x\partial y}+\tfrac{1}{2}F_{2_0}\left(\frac{\partial^2 u'}{\partial y^2}+\frac{\partial^2 v'}{\partial x\partial y}\right)+\frac{1}{2}\frac{\partial U}{\partial y}\left(\frac{\partial F_2}{\partial \nu}\bigg|_0\frac{\partial \nu'}{\partial y}+\frac{\partial F_2}{\partial T}\bigg|_0\frac{\partial T'}{\partial y}\right), \quad (3.1)$$

$$\nu_0\left(\frac{\partial v'}{\partial t}+U\frac{\partial v'}{\partial x}\right) = +\tfrac{1}{2}F_{2_0}\left(\frac{\partial^2 u'}{\partial x\partial y}+\frac{\partial^2 v'}{\partial x^2}\right)+\frac{1}{2}\frac{\partial U}{\partial y}\left(\frac{\partial F_2}{\partial \nu}\bigg|_0\frac{\partial \nu'}{\partial x}+\frac{\partial F_2}{\partial T}\bigg|_0\frac{\partial T'}{\partial x}\right)$$
$$-F_{1_0}\frac{\partial T'}{\partial y}-T_0\frac{\partial F_1}{\partial \nu}\bigg|_0\frac{\partial \nu'}{\partial y}+(\alpha_0-\tfrac{1}{3}F_{2_0})\frac{\partial^2 u'}{\partial x\partial y}+(\alpha_0+\tfrac{2}{3}F_{2_0})\frac{\partial^2 v'}{\partial y^2}, \quad (3.2)$$

$$\tfrac{3}{2}\nu_0\left(\frac{\partial T'}{\partial t}+U\frac{\partial T'}{\partial x}\right) = -\left(\frac{\partial u'}{\partial x}+\frac{\partial v'}{\partial y}\right)p_{xx_0}-\left(\frac{\partial v'}{\partial x}+\frac{\partial u'}{\partial y}\right)p_{xy_0}$$
$$+\tfrac{1}{2}F_{2_0}\frac{\partial U}{\partial y}\left(\frac{\partial u'}{\partial y}+\frac{\partial v'}{\partial x}\right)+\frac{1}{2}\left(\frac{\partial U}{\partial y}\right)^2\left(\frac{\partial F_2}{\partial \nu}\bigg|_0\nu'+\frac{\partial F_2}{\partial T}\bigg|_0 T'\right)$$
$$-\frac{\partial \gamma}{\partial \nu}\bigg|_0\nu'-\frac{\partial \gamma}{\partial T}\bigg|_0 T'+K_0\left(\frac{\partial^2 T'}{\partial x^2}+\frac{\partial^2 T'}{\partial y^2}\right). \quad (3.3)$$

We now consider possible solutions to (2.34) and (3.1)–(3.3) for the perturbation solids fraction ν', velocities u' and v', and the perturbation temperature T'.

3.1. *Shear-induced turning of wavenumber vector*

In a review of shear-flow turbulence, Phillips (1969) has discussed simple models (cf. Moffatt 1967) to consider the maintenance of disturbances or turbulent components interacting with the mean flow for (inviscid) incompressible, uniform shear flows. Some simple solutions had the form of Fourier modes in which the wavenumber vector was turned by the mean shear flow. We also note that in computer simulations of suspensions of particles, Brady & Bossis (1988) show clusters or bands (see their figure 6, p. 138) that were rotated 'more or less en masse' owing to the presence of the mean shear. Here we shall examine the stability of similar modes of the form

$$\left.\begin{aligned}\nu' &= \hat{\nu}(t)\exp \mathrm{i}(\boldsymbol{k}(t)\cdot\boldsymbol{x}), \quad u' = \hat{u}(t)\exp \mathrm{i}(\boldsymbol{k}(t)\cdot\boldsymbol{x}),\\ v' &= \hat{v}(t)\exp \mathrm{i}(\boldsymbol{k}(t)\cdot\boldsymbol{x}), \quad T' = \hat{T}(t)\exp \mathrm{i}(\boldsymbol{k}(t)\cdot\boldsymbol{x}).\end{aligned}\right\} \quad (3.4)$$

where $\quad \boldsymbol{x} = [x,y], \quad \boldsymbol{k}(t) = [k_x, k_y] = [k_x(0), k_y(0)-tk_x(0)], \quad (3.5)$

and $k_x(0)$ and $k_y(0)$ are the components of the wavenumber vector at the initial time $t=0$. Note that the x-component remains constant at its initial value $k_x(0)$ but that the y-component varies linearly with time t. The lines of constant phase move closer

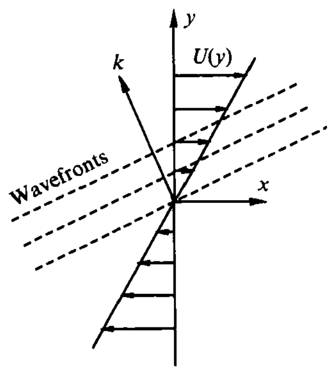

FIGURE 2. Definition of coordinate system and rotation of wavenumber vector by action of mean shear.

together with increasing time and rotate so that they become more parallel to the x-axis (see figure 2). Substituting (3.4) in the conservation equations (2.34) and (3.1)–(3.3) yields the following set of equations for the amplitudes $\hat{\nu}$, $\hat{u}$, $\hat{v}$, and $\hat{T}$.

$$\dot{\hat{\nu}} = -\mathrm{i}\nu_0(k_x\hat{u}+k_y\hat{v}), \tag{3.6}$$

$$\dot{\hat{u}} = -\frac{\mathrm{i}}{\nu_0}\left[T_0\frac{\partial F_1}{\partial \nu}\bigg|_0 k_x - \frac{1}{2}\frac{\partial F_2}{\partial \nu}\bigg|_0 k_y\right]\hat{\nu} - \frac{1}{\nu_0}[(\alpha_0+\tfrac{2}{3}F_{2_0})k_x^2+\tfrac{1}{2}F_{2_0}k_y^2]\hat{u}$$
$$-\frac{1}{\nu_0}[(\alpha_0-\tfrac{1}{3}F_{2_0}+\tfrac{1}{2}F_{2_0})k_xk_y+\nu_0]\hat{v} - \frac{\mathrm{i}}{\nu_0}\left[F_{1_0}k_x - \frac{1}{2}\frac{\partial F_2}{\partial T}\bigg|_0 k_y\right]\hat{T}, \tag{3.7}$$

$$\dot{\hat{v}} = -\frac{\mathrm{i}}{\nu_0}\left[T_0\frac{\partial F_1}{\partial \nu}\bigg|_0 k_y - \frac{1}{2}\frac{\partial F_2}{\partial \nu}\bigg|_0 k_x\right]\hat{\nu} - \frac{1}{\nu_0}[\alpha_0-\tfrac{1}{3}F_{2_0}+\tfrac{1}{2}F_{2_0}]k_xk_y\hat{u}$$
$$-\frac{1}{\nu_0}[(\alpha_0+\tfrac{2}{3}F_{2_0})k_y^2+\tfrac{1}{2}F_{2_0}k_x^2]\hat{v} - \frac{\mathrm{i}}{\nu_0}\left[F_{1_0}k_y - \frac{1}{2}\frac{\partial F_2}{\partial T}\bigg|_0 k_x\right]\hat{T}, \tag{3.8}$$

$$\dot{\hat{T}} = -\frac{2}{3\nu_0}\left[\frac{\partial \gamma}{\partial \nu}\bigg|_0 - \frac{1}{2}\frac{\partial F_2}{\partial \nu}\bigg|_0\right]\hat{\nu} - \frac{2\mathrm{i}}{3\nu_0}[\bar{p}_0k_x - F_{2_0}k_y]\hat{u}$$
$$-\frac{2\mathrm{i}}{3\nu_0}[\bar{p}_0k_y - F_{2_0}k_x]\hat{v} - \frac{2}{3\nu_0}\left[-\frac{1}{2}\frac{\partial F_2}{\partial T}\bigg|_0 + \frac{\partial \gamma}{\partial T}\bigg|_0 + K_0(k_x^2+k_y^2)\right]\hat{T}. \tag{3.9}$$

We now examine the initial growth (or decay) rates of the amplitudes $\hat{\nu}$, $\hat{u}$, $\hat{v}$, and $\hat{T}$ at time $t = 0$ for arbitrary initial values of components $k_x(0)$ and $k_y(0)$ of the wavenumber vector. For example, we can then write

$$\left.\begin{aligned} \hat{\nu} &= \breve{\nu}\exp(-\mathrm{i}nt), & \hat{u} &= \breve{u}\exp(-\mathrm{i}nt), \\ \hat{v} &= \breve{v}\exp(-\mathrm{i}nt), & \hat{T} &= \breve{T}\exp(-\mathrm{i}nt), \end{aligned}\right\} \tag{3.10}$$

where $\breve{\nu}$, $\breve{u}$, etc. are constants. Substituting (3.10) into (3.6)–(3.9) yields a system of four equations in the form $(A-nI)X$ where X represents the four numbers $\breve{\nu}$, $\breve{u}$, $\breve{v}$, and $\breve{T}$. This system has non-trivial roots only if $|A-nI| = 0$. When this is expanded it yields a fourth-degree polynomial characteristic equation for the complex wave frequency n. The real part of n is the wave frequency n_r, and the imaginary part n_i is the growth rate. We want to determine the most unstable modes that occur and hence we seek the largest value of the growth rate n_i. The analysis is extremely

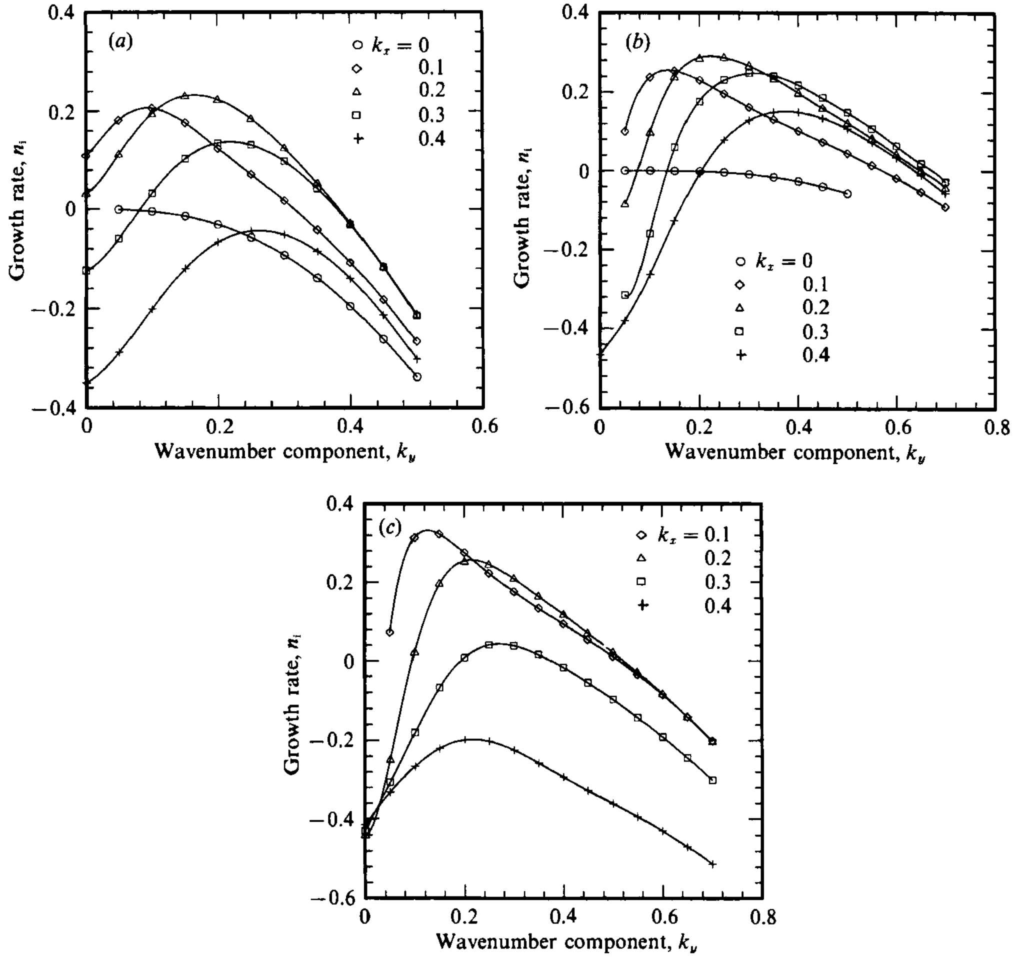

FIGURE 3. Initial growth rate n_i versus the y-component of the initial wavenumber, $k_y(0)$, for various constant values of the x-component of the initial wavenumber, $k_x(0)$, and for a coefficient of restitution $e = 0.8$. Modes correspond to case of shear-induced turning of wavenumber vector. (*a*) $\nu_0 = 0.1$, (*b*) $\nu_0 = 0.3$, (*c*) $\nu_0 = 0.5$.

lengthy and complicated and was carried out using symbolic algebra packages. Initial studies were performed with REDUCE 3.3 (Hearn 1987, Rayna 1987) running on an Acorn Springboard RISC coprocessor board mounted in an MS-DOS 80386 microcomputer. Even before the functions such as α_0, F_{1_0}, F_{2_0}, etc. that appeared in (3.6)–(3.9) are written out in full and differentiations of them with respect to ν and T are performed, the polynomial for n is hundreds of lines in length. In these initial studies the subsequent numerical determination of the roots of the complex wave frequency n were determined with the symbolic computation package DERIVE 2.01 (Rich, Rich & Stoutmeyer 1990) since it handles complex algebra and arithmetic nicely. This work was later checked using the symbolic package MATHEMATICA (Wolfram 1991) running on a NeXTstation; this package was able to handle both the algebraic manipulation and the numerical evaluations effectively.

Some typical results are shown in figure 3 for a coefficient of restitution $e = 0.8$ and for solids fractions $\nu_0 = 0.1$, 0.3 and 0.5. If the growth rate n_i is positive, the perturbations will grow and the flow is unstable; if n_i is negative, the flow is stable and disturbances decay in time. The larger the (algebraic) value of n_i, the more unstable (or the less stable) is the flow. Figure 3 shows the initial growth rate n_i plotted versus the initial wavenumber component $k_y(0)$ for constant values of the x-component of wavenumber, $k_x(0)$, and for constant values of mean solids fraction ν_0. Note that the flows are most unstable when the initial wavenumber vector components $k_x(0) \approx k_y(0)$, i.e. when the initial wavenumber vector is inclined at approximately $\frac{1}{4}\pi$ to the x-axis. It may also be seen that, in general, when the initial wavenumber vector is inclined somewhat greater than $\frac{1}{4}\pi$ (i.e. when $k_y(0) > k_x(0)$), the flow becomes more unstable with increasing time as the wavenumber vector is rotated by the mean flow and k_y decreases (cf. (3.5)). When the initial wavenumber vector is inclined at an angle somewhat less than $\frac{1}{4}\pi$ with respect to the x-axis (i.e. when $k_y(0) < k_x(0)$), the flow becomes more stable with increasing time. Similar behaviour is found for other values of e. For this case of $e = 0.8$, it may be seen by comparing figures 3 (*a*), 3 (*b*) and 3 (*c*) that for the most part the flows tend to be more stable at very high- and low-solids fractions and least stable at moderate concentrations.

It should also be noted that in almost all cases considered, n_r (the real part of the complex frequency n) was zero, corresponding to waves with a zero phase velocity (i.e. 'standing waves' whose wavenumber vector is rotated by the mean shear flow).

Figure 4 shows the (algebraically) largest values of the growth rate n_i plotted versus solids fraction for constant values of initial wavenumbers $k_x(0) = k_y(0)$ which were seen to be the approximate conditions for the flows to be the most unstable or least stable. Results are shown for three values of coefficient of restitution; $e = 0.9$, 0.8, and 0.5. As was noted previously, it is seen that the flows tend to be most unstable for long wavelength disturbances and stable for short wavelength disturbances. Figure 4 shows again that, in general, for constant values of $k_x(0) = k_y(0)$, the flows are most unstable at moderate values of solids fractions and tend to be more stable at both high and low concentrations. There is a small dependence of n_i on coefficient of restitution e. At larger wavelengths, decreasing e increases the tendency for the flow to be unstable.

We can understand physically why flows might be most unstable when the wavenumber vector of the perturbations is inclined at $\frac{1}{4}\pi$ to the x-coordinate axis if we recall that the compressive axis of the present simple shear flow is aligned at $\frac{3}{4}\pi$ to the x-coordinate axis and the extensional axis is oriented $\frac{1}{4}\pi$ from it. We can visualize how discrete particles would tend to be squeezed together so as to collect along the compressive axis and be 'pulled apart' along the extensional direction. There would be a tendency to develop bands, the axes of which would be inclined at $\frac{3}{4}\pi$ from the x-axis. The computer simulations of Brady & Bossis (1988, cf. figure 6, p. 138) clearly show the development of these kinds of bands. They noted that the microstructure appeared to be rotated 'more or less en masse' by the mean shear. This appears to be much like the shear-induced turning of the wave modes that have been considered here.

The above results and trends seem to be consistent with the simulations of Hopkins & Louge (1991) as much as the trends in their simulations can be discerned clearly. However, one must be careful to distinguish between the present results which predict the likelihood of linear stability (or instability) and the results of Hopkins & Louge which determined the extent (and intensity) of well-developed (?) inhomogeneities in the flows. Obviously the two situations are related, but not necessarily the same. Hopkins & Louge stated that wavelength of the microstructures (inhomogeneities) generally increased with the size of the periodic computational

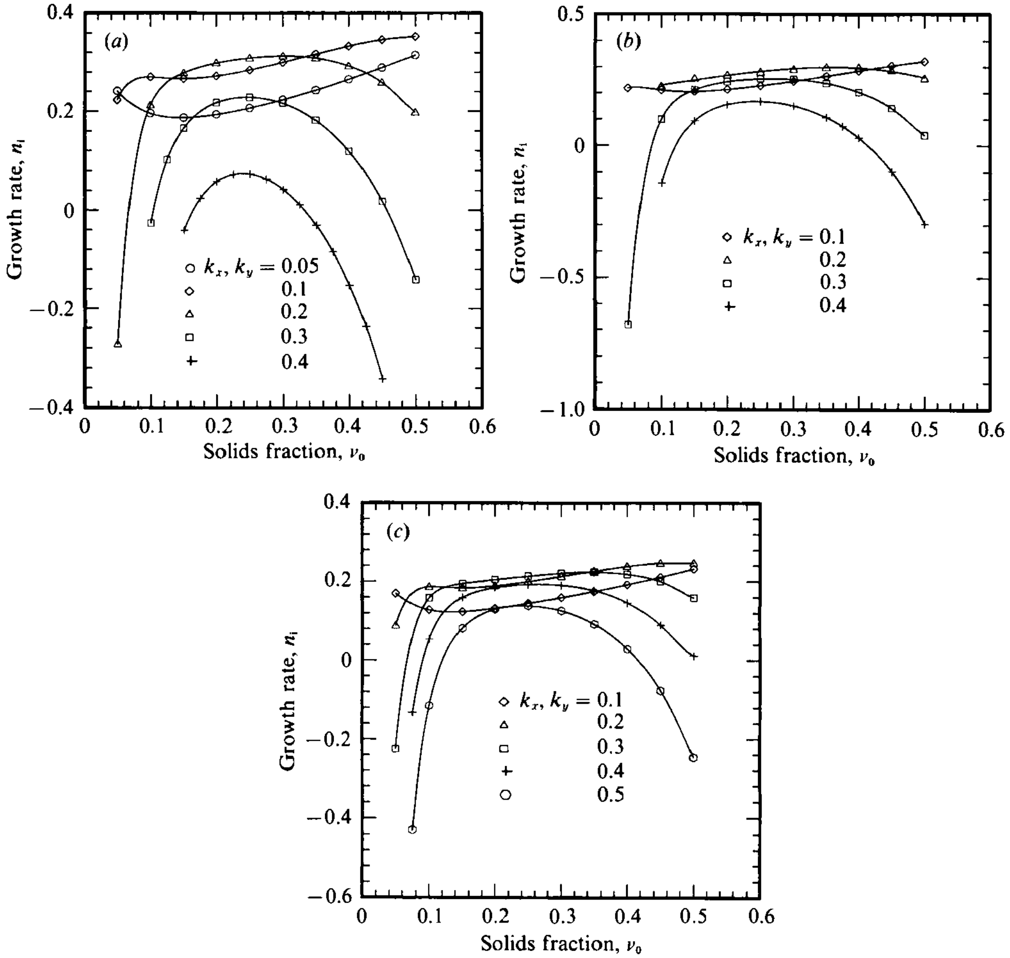

FIGURE 4. Growth rate n_i versus solids fraction ν_0 for constant values of initial wavenumber components $k_x(0) = k_y(0)$ and coefficient of restitution e; (a) $e = 0.9$, (b) $e = 0.8$, (c) $e = 0.5$.

domain; and that as the size of the periodic computational domain decreased the microstructures tended to disappear. Furthermore, increasing e tended to forestall the growth of the microstructures.

The use of periodic boundary conditions in the computer simulations will effectively 'fix' the wavelength. Since, in general, the long wavelengths are predicted to be the most unstable, it would seem likely that the dominant wavelength of the unstable perturbations would correspond to the size of the periodic box used in the simulations. Thus, computations performed using 'small boxes' and small numbers of particle can be stable, while 'larger' boxes involving larger numbers of particles are more likely to be unstable. Superposition of plane wave Fourier modes in the case of the shear-induced wavenumber turning case could produce the complex structures that seem to be present in the disk simulations of Hopkins & Louge (1991). At low density the observed non-homogenieties appear to be quite strong; it is possible that they might be generated or enhanced by nonlinear interactions.

4. Concluding remarks

The present work has examined the linear stability of a uniform granular shear flow of inelastic spherical particles. It should be noted that only some particular forms of perturbation solutions have been examined. There may be others similar to those considered in studies of the stability of viscous fluid boundary layers (e.g. Betchov & Criminale 1967).

Flows at high mean solids fraction often involve shearing in layers of only a few particle layers thick. Under these conditions the instabilities and resulting inhomogeneities in density, granular temperature and velocities of the kind considered in the present paper might not be so likely. However, other kinds of inhomogeneities, such as spatial and temporal stress fluctuations, particle clustering and break-up which result in mean density fluctuations, the formation of columns of particles in contact, jamming and bridging of particles, occur. They can be observed in computer simulations and also inferred from physical shear cell experiments (Savage & Sayed 1984). On the other hand, for flows at lower densities when the shear regions are much thicker, the instabilities discussed in the present paper are expected to significantly affect the overall flow dynamics. Flows at low mean solids fractions also permit the possibility of density fluctuations of larger magnitude than are possible at high mean densities. This increases the likelihood of important nonlinear effects. It would be interesting (but certainly very difficult) to consider nonlinear wave interactions in these kinds of granular flows.

The present work has considered only the onset of instability in a granular shear flow. Both computer simulations and shear cell experiments indicate that fluctuations of significant magnitude in stresses, solids fraction, etc. can be maintained. There are not only the obvious short-time fluctuations associated with the individual particle motions, but also those which involve longer timescales. Here we can think of analogies to the fine grain turbulence and large-scale coherent structures that are observed in turbulent fluid flows (Liu 1990). Previous solutions to boundary-value problems (using constitutive relations derived from granular flow kinetic theories) have been based upon the assumption of homogeneous slowly varying flow fields. Some attempts should be made to include turbulent-like fluctuations (whose spatial and temporal scales are larger than those associated with the individual particle fluctuations) in the derivation of constitutive equations and examine the effects of their inclusion on quantities like mean stresses, energy fluxes, etc.

This work was supported by an Operating Grant from the Natural Sciences and Engineering Research Council of Canada (NSERC).

REFERENCES

Bagnold, R. A. 1954 Experiments on a gravity free dispersion of large solid spheres in a Newtonian fluid under shear. *Proc. R. Soc. Lond.* A**225**, 49–63.

Barnes, H. A. 1989 Shear-thickening ('Dilatancy') in suspensions of nonaggregating solid particles dispersed in Newtonian liquids. *J. Rheol.* **33**, 329–366.

Batchelor, G. K. & Janse van Rensburg, R. W. 1986 Structure formation in bidisperse sedimentation. *J. Fluid Mech.* **166**, 379–407.

Betchov, R. & Criminale, W. O. 1967 *Stability of Parallel Flows*. Academic.

Brady, J. F. & Bossis, G. 1988 Stokesian dynamics. *Ann. Rev. Fluid Mech.* **20**, 111–157.

CAMPBELL, C. S. 1989 The stress tensor for simple shear flows of a granular material. *J. Fluid Mech.* **203**, 449–473.

CAMPBELL, C. S. 1990 Rapid granular flows. *Ann. Rev. Fluid Mech.* **22**, 57–92.

CAMPBELL, C. S. & BRENNEN, C. E. 1985 Computer simulation of granular shear flows. *J. Fluid Mech.* **151**, 167–188.

CAMPBELL, C. S. & GONG, A. 1986 The stress tensor in a two-dimensional granular shear flow. *J. Fluid Mech.* **164**, 107–125.

CARNAHAN, N. F. & STARLING, K. E. 1969 Equations of state for non-attracting rigid spheres. *J. Chem. Phys.* **42**, 635–636.

GREEN, D. & HOMSY, G. M. 1987 Instabilities in self-fluidized beds – I: Theory. *Intl J. Multiphase Flow* **13**, 443–457.

GUTT, G. M. & HAFF, P. K. 1988 Boundary conditions on continuum theories of granular flow. Brown Bag Preprint Series BB-70, Division of Physics, Mathematics, and Astronomy, Caltech, 24 pp.

HAFF, P. K. 1983 Grain flow as a fluid-mechanical phenomenon. *J. Fluid Mech.* **134**, 401–430.

HAFF, P. K. 1986 A physical picture of kinetic granular flow. *J. Rheol.* **30**, 931–948.

HANES, D. M., JENKINS, J. T. & RICHMAN, M. W. 1988 The thickness of steady plane shear flows of circular disks driven by identical boundaries. *J. Appl. Mech.* **110**, 969–974.

HEARN, A. C. 1987 *REDUCE* Users Manual, Version 3.3. Rand Publication CP78, Rev. 7/87, The Rand Corporation, Santa Monica.

HOPKINS, M. A. & LOUGE, M. Y. 1991 Inelastic microstructure in rapid granular flows of smooth disks. *Phys. Fluids* A **3**, 47–57.

HOPKINS, M. A. & SHEN, H. 1988 A Monte-Carlo simulation of a rapid simple shear flow of granular materials. In *Micromechanics of Granular Materials* (ed. M. Satake & J. T. Jenkins), pp. 349–358. Elsevier.

HUI, K., HAFF, P. K., UNGAR, J. E. & JACKSON, R. 1984 Boundary conditions for high shear grain flows. *J. Fluid Mech.* **145**, 223–233.

JACKSON, R. 1985 Hydrodynamic stability of fluid particle systems. In *Fluidization* (ed. J. F. Davidson, R. Clift & D. Harrison). Academic.

JENKINS, J. T. 1987*a* Balance laws and constitutive relations for rapid flows of granular materials. In *Constitutive Models of Deformations* (ed. J. Chandra & R. Srivastav), p. 109. Philadelphia: SIAM.

JENKINS, J. T. 1987*b* Rapid flows of granular materials. In *Non-classical Continuum Mechanics: Abstract Techniques and Applications* (ed. R. J. Kops & A. A. Lacey), pp. 213–224. Cambridge University Press.

JENKINS, J. T. & RICHMAN, M. W. 1985 Grad's 13-moment system for a dense gas of inelastic spheres. *Arch. Rat. Mech. Anal.* **87**, 355–377.

JENKINS, J. T. & RICHMAN, M. W. 1986 Boundary conditions for plane flows of smooth nearly elastic, circular disks. *J. Fluid Mech.* **171**, 53–69.

JENKINS, J. T. & SAVAGE, S. B. 1983 A theory for the rapid flow of identical, smooth, nearly elastic particles. *J. Fluid Mech.* **130**, 186–202.

JOHNSON, P. C. & JACKSON, R. 1987 Frictional–collisional constitutive relations for granular materials, with application to plane shearing. *J. Fluid Mech.* **176**, 67–93.

KYTÖMAA, H. K. & BRENNEN, C. E. 1990 Kinematic instability of three-component flows. *Intl J. Multiphase Flow* (to be submitted).

LEES, A. W. & EDWARDS, S. F. 1972 The computer study of transport processes under extreme conditions. *J. Phys.* C **5**, 1921–9.

LIU, J. T. C. 1990 Coherent structures in transitional and turbulent free shear flows. *Ann. Rev. Fluid Mech.* **21**, 285–315.

LUN, C. K. K., SAVAGE, S. B., JEFFREY, D. J. & CHEPURNITY, N. 1984 Kinetic theories for granular flow: inelastic particles in Couette flow and slightly inelastic particles in a general flowfield. *J. Fluid Mech.* **140**, 223–256.

MOFFATT, H. K. 1967 The interaction of turbulence with strong wind shear. In *Atmospheric Turbulence and Radio Wave Propagation* (ed. A. M. Yaglom & V. I. Tatarsky), pp. 135–56. Moscow: Nauka.

PHILLIPS, O. M. 1969 Shear-flow turbulence. *Ann. Rev. Fluid Mech.* **1**, 245–64.

RAYNA, G. 1987 *REDUCE, Software for Algebraic Computation.* Springer.

RICH, A., RICH, J. & STOUTEMYER, D. 1990 DERIVE, Version 2, User Manual. Soft Warehouse, Honolulu, Hawaii.

RICHMAN, M. W. 1988 Boundary conditions based upon a modified Maxwellian velocity distribution for flows of identical, smooth nearly elastic, spheres. *Acta Mech.* **75**, 227–240.

RICHMAN, M. W. 1989 The source of second moment in dilute granular flows of highly inelastic spheres. *J. Rheol.* **33**, 1293–1306.

RICHMAN, M. W. & CHOU, C. S. 1988 Boundary effects on granular shear flows of smooth disks. *Z. angew. Math. Phys.* **39**, 885–901.

SAVAGE, S. B. 1983 Granular flows down rough inclines – review and extension. *Mechanics of Granular Materials: New Models and Constitutive Relations* (ed. J. T. Jenkins & M. Satake), pp. 261–282. Elsevier.

SAVAGE, S. B. 1984 The mechanics of rapid granular flows. *Adv. Appl. Mech.* **24**, 289–366.

SAVAGE, S. B. 1989 Flow of granular materials. In *Theoretical and Applied Mechanics* (ed. P. Germain, M. Piau & D. Caillerie), pp. 241–266. Elsevier.

SAVAGE, S. B. 1991 Numerical simulations of Couette flow of granular materials; spatio-temporal coherence and $1/f$ noise. In *Physics of Granular Media* (ed. J. Dodds & D. Bideau). New York: Nova Scientific (in press).

SAVAGE, S. B. & JEFFREY, D. J. 1981 The stress tensor in a granular flow at high shear rates. *J. Fluid Mech.* **110**, 255–272.

SAVAGE, S. B. & SAYED, M. 1984 Stresses developed by dry cohesionless granular materials sheared in an annular shear cell. *J. Fluid Mech.* **142**, 391–430.

SHEN, H. & ACKERMANN, N. L. 1982 Constitutive relationships for fluid–solid mixtures. *J. Engng Mech. Div. ASCE* **108**, 748–763.

SHEN, H. & ACKERMANN, N. L. 1984 Constitutive equations for a simple shear flow of disk shaped granular material. *Intl J. Engng Sci.* **22**, 829–843.

SHLESINGER, M. F. & WEST, B. 1988 $1/f$ versus $1/f^a$ noise. *Random Fluctuations and Pattern Growth* (ed. H. E. Stanley & N. Ostrowsky), pp. 320–324. Dordrecht: Kluwer Academic.

VOSS, R. F. 1988 Fractals in nature: From characterization to simulation. In *The Science of Fractal Images* (ed. H.-O. Peitgen & D. Saupe), pp. 21–70. Springer.

WALTON, O. R. & BRAUN, R. L. 1986*a* Stress calculations for assemblies of inelastic spheres in uniform shear. *Acta Mech.* **63**, 73–86.

WALTON, O. R. & BRAUN, R. L. 1986*b* Viscosity and temperature calculations for assemblies of inelastic frictional disks. *J. Rheol.* **30**, 949–980.

WALTON, O. R., BRAUN, R. L., MALLON, R. G. & CERVELLI, D. M. 1987 Particle-dynamics calculations of gravity flow of inelastic, frictional spheres. In *Micromechanics of Granular Materials* (ed. M. Satake & J. T. Jenkins), pp. 153–162. Elsevier.

WALTON, O. R., KIM, H. & ROSATO, A. 1991 Micro-structure and stress differences in shearing flows. In *Mechanics Computing in 1990's and Beyond* (ed. H. Adeli & R. L. Sierakowski), Vol. 2, pp. 1249–1253. ASCE.

WEILAND, R. H., FESSAS, Y. P. & RAMARAO, B. V. 1984 On instabilities arising during sedimentation of two-component mixtures of solids. *J. Fluid Mech.* **142**, 383–389.

WOLFRAM, S. 1991 *MATHEMATICA, A system for doing mathematics by computer* (2nd edn). Addison Wesley.